Journal of the Korean Physical Society, Vol. 51, No. 1, July 2007, pp. 306∼311

Chirality Assignment of Micelle-Suspended Single-Walled Carbon Nanotubes Using Coherent Phonon Oscillations

Yong-Sik Lim*
Department of Applied Physics, Konkuk University, Chungju 380-701 and Department of Electrical and Computer Engineering, Rice University, Texas 77005, U.S.A.

Ki-Ju Yee and Ji-Hee Kim
Department of Physics, Chungnam National University, Daejeon 305-764

Erik H. Hároz, Jonah Shaver and Junichiro Kono
Department of Electrical and Computer Engineering, Rice University, Texas 77005, U.S.A. and Carbon Nanotechnology Laboratory, Rice University, Texas 77005, U.S.A.

Stephen K. Doorn
Division of Chemistry, Chemical Science and Engineering, Los Alamos Laboratory, NM 87545, U.S.A.

Robert H. Hauge and Richard E. Smalley
Carbon Nanotechnology Laboratory, Rice University, Texas 77005, U.S.A.

(Received 31 January 2007)

We report on a new high-resolution optical spectroscopy, coherent phonon measurement, for determining the chiral index of carbon nanotubes. Using femtosecond pump-probe spectroscopy, we demonstrate the real-time observation of lattice vibrations in individualized single-walled carbon nanotubes in an aqueous surfactant solution. Almost all available radial breathing modes in the Fourier transform spectrum from coherent phonon oscillations are well-resolved with less ambiguity in comparison to continuous-wave resonant Raman scattering.

PACS numbers: 78.47.+p, 63.22.+m, 78.66.Tr
Keywords: Single-walled carbon nanotubes, Coherent phonon oscillations, Chirality assignment

I. INTRODUCTION

Single-walled carbon nanotubes (SWNTs) are quasi-one dimensional molecules of carbon with uniquely simple crystal structures. Their dimensionality provides a playground for studying the dynamics of confined electrons and phonons and their interplay [1]. Because the electronic and the optical properties of nanotubes vary greatly with their chiral indices (n, m), which can be directly related to their respective diameter (d) and chiral angle (θ), the precise determination of the chiral index is a major focus of basic and applied nanoscience. Direct and indirect techniques, such as high-resolution microscopy and continuous-wave (CW) optical spectroscopy, respectively, have been widely utilized to investigate the precise structure of nanotubes. While nanoscale microscopies like transmission electron microscopy (TEM), scanning electron microscopy (SEM), scanning tunneling microscopy (STM), and atomic force microscopy (AFM) make it possible to monitor individual nanotubes with high resolution at the nano-scale and in some cases even directly determine the (n, m) index, such techniques demand a high degree of skill and experience and delicate sample preparation to produce high quality, useful images. Also because of the limited field of view at such high magnification, taking sufficient images of a statistically representative group of nanotubes for a given sample is time consuming, making bulk characterization difficult [2–6]. CW spectroscopies, such as resonant Raman scattering, optical absorption, and photoluminescence excitation, have been widely used for the structural assignment of SWNT species [7–10]. In particular, CW optical studies of SWNTs have produced a variety of intriguing phenomena, including phonon-assisted photoluminescence, strongly bound excitions, and chirality-dependent resonant Raman scattering, all results of the interaction between excited

*E-mail: yslim@kku.ac.kr; Fax: +82-43-851-4169

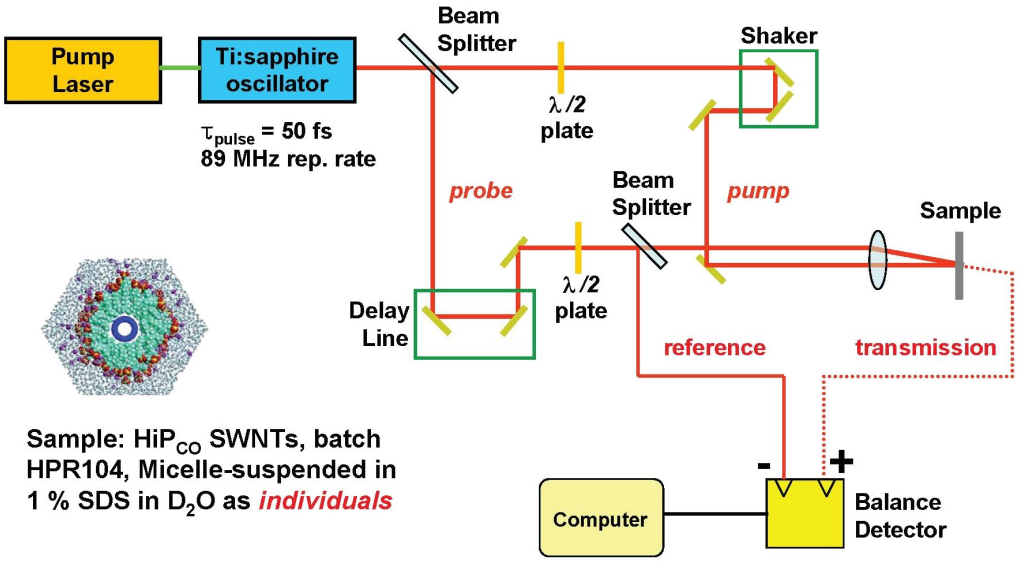

Fig. 1. Degenerate pump-probe experimental setup. Pulses of 50 fs in pulsewidth were divided into a pump beam and a probe beam. Coherent phonon oscillations were obtained by detecting the differential transmittance of the probe beam passing through a ∼1 mm quartz cell containing micelle-suspended HiPco single-walled carbon nanotubes in aqueous solutions [22]. The reference beam was split off from the probe beam and sent to a detector in a balanced photodetector pair.

electronic states and phonons [11–18]. However, recent works have shown that these optical methods are sometimes not sensitive enough to clearly resolve all chiralities present in samples and can even exhibit different chirality dependences in their spectral intensity, depending on the method [9,12,19,20].

Recently, we have generated and detected coherent lattice vibrations in SWNTs corresponding to the radial breathing mode (RBM) by using femtosecond optical pulses and a pump-probe technique [21]. Here, we report on the use of coherent phonon measurement of such high spectral resolution to enable the assignment of the chiral indices of SWNTs without ambiguity. We also show how to observe real-time lattice vibrations in detail and present a direct comparison between the CP spectrum and the CW RRS spectrum.

II. EXPERIMENTS

The sample was made from HiPco SWNTS (batch HPR104) with a diameter range of 0.7 ∼ 1.3 nm. As Figure 1 shows, the SWNTs were suspended as individuals in a solution of 1 % sodium dodecyl sulfate in D_2O, as described in detail elsewhere [22]. We performed degenerate pump-probe measurements in a quartz cell with an optical path length of 1 mm by using ∼50 fs pulses from a mode-locked Ti:Sapphire laser (Kapteyn-Murnane Labs) with a center wavelength at 830 nm and a repetition rate of 89 MHz. As Figure 1 shows, we used a noncollinear geometry with a pump beam diameter of ∼1 mm, which was focused onto the sample by using a lens with a 10 cm focal length. The average pump power was kept small (∼20 mW) to avoid the thermal-lens effect in the D_2O solvent. To detect small photoinduced changes in probe beam transmission, we used a balanced photodetector pair (New Focus Inc, Nirvana detector), in which a photodiode was illuminated by a weak reference beam split from the probe beam, together with a fast-scanning 'shaker' delay stage with a sinusoidal motion of 10 Hz. The maximum delay was ∼20 ps, which corresponded to a spectral resolution of about 1.7 cm^{-1} in the frequency domain. In a scan, three thousand data points were collected with a high speed data acquisition card with a 3 MHz sample rate and subsequently added and averaged with new data from each scan to enhance the signal-to-noise ratio of the collected data. The smallest detectable differential transmission, $\Delta T/T$, was $\sim 10^{-5}$. In the CW resonance Raman scattering experiment, the excitation source was a Spectra Physics model 3900 Ti:Sapphire laser with a CW mode power of 15 mW at the same sample. Signal collection was done using a Spex model 1877 triple monochromator and Princeton Instruments CCD camera with a 5 cm^{-1} resolution and a 5 minute integration time. The collected spectra were background- and baseline-subtracted to remove Rayleigh scattering and the nanotube fluorescence signal and were corrected for the instrument response and the ν^4 dependence. The Raman shift was calibrated using an acetaminophen standard.

III. RESULTS AND DISCUSSION

Figure 2(a) shows the raw pump-probe data taken for our SWNT sample with 50 fs pulses at a center wave-

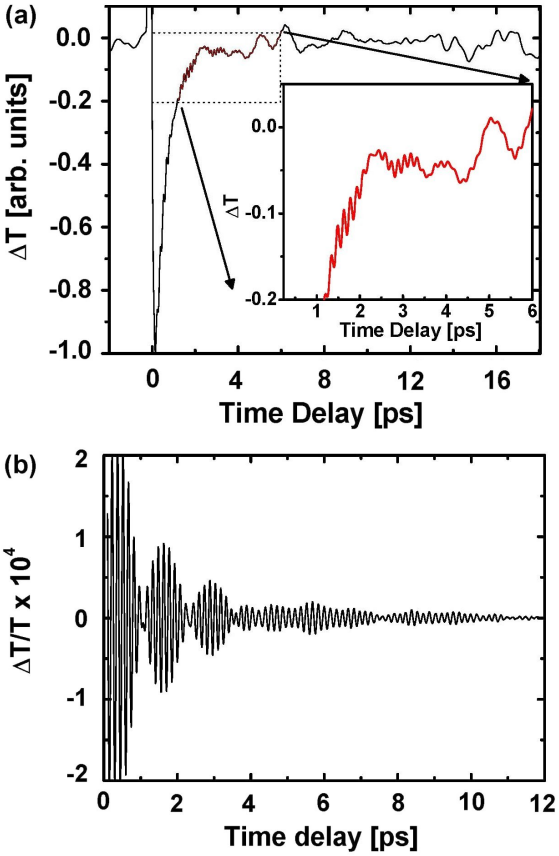

Fig. 2. (a) Raw pump-probe data in the time domain taken with 50 fs pulses with a center photon wavelength at 830 nm. The inset is a zoom-in of the data taken between 1.2 ps and 6 ps, highlighting the coherent phonon oscillations within the transmitted signal. (b) Coherent phonon oscillations, exhibiting a strong beating pattern, excited and measured at 830 nm center photon wavelength in a normalized transmittance scale. The trace is offset for clarity.

length of 830 nm. A large electronic contribution is seen at zero delay between the pump and the probe beams and is followed by weaker decaying oscillatory components only at positive delay. The slowly varying background of the raw data at positive delay is due to the decaying electronic contribution, beam fluctuation, and working-off of the pump beam reflected from the shaker, as shown in the inset of Figure 2(a). Figure 2(b) shows coherent phonon oscillations from baseline-subtracted raw data to remove the slowly varying contributions. The amplitude of the oscillations in terms of normalized differential transmission was as strong as $\sim 10^{-4}$ near zero delay, which is comparable or superior to optical phonon oscillations of zinc-blende semiconductors, like GaAs and ZnSe [23,24]. The time trace exhibits a strong beating pattern, indicating the presence of a superposition of multiple oscillations of different frequencies with similar, but somewhat different, decay times. As we described in our previous study, the beating pattern sensitively changes with the excitation photon energy, implying that the CP oscillations are attributed to RBMs, which are resonantly enhanced by pulses with a broad spectrum commensurate with their unique electronic transitions, as in CW resonant Raman scattering (RRS). The decay time of the CP oscillations was ~5 ps (2 ps for the fast ones and 9 ps for the slow ones), which is also the same order as the LO and the Ag modes of bulk semiconductors like GaAs and GaN, respectively [23,25].

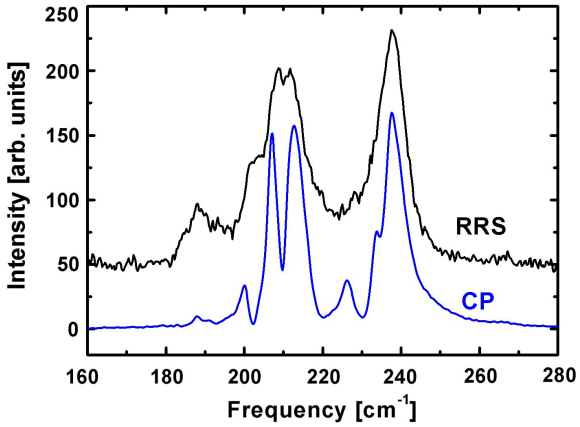

Fig. 3. Comparison between the CW resonant Raman scattering spectrum (upper black trace) and the Fourier-transformed spectrum (lower blue trace) from coherent phonon oscillations for the same HiPco sample (batch HPR 104) at an excitation energy of 1.486 eV (830 nm). The coherent phonon spectrum is not only consistent with the CW resonant Raman scattering spectrum but also shows sharper features and a higher S/N ratio. The traces are offset for clarity.

To investigate what kinds of RBMs are excited, we took a fast Fourier-transform (FFT) of the time-domain oscillations to produce the CP spectrum and compared it with the CW RRS spectrum, as shown in Figure 3. The main peak positions coincide well between both spectra, indicating that the beating oscillations are, indeed, due to coherent lattice vibrations of the RBMs. It should be noticed that it is possible for the peak position in the CP spectrum to deviate slightly from that of the RRS spectrum due to the double peak feature of the CP spectrum, which is attributed to ultrafast band gap oscillations produced by RBM-induced diameter oscillations, which are uniquely enhanced in the CP signal detection process [21]. However, this double peak feature in the CP spectrum can be applied for precise determination of the phonon frequency. Compared with the FFT spectrum of CP signal and the RRS spectrum, we find that CP data show narrower phonon line widths and excellent resolution, allowing blended peaks to appear as distinct features. The CP spectrum shows a better signal-to-noise ratio of twenty times that of CW Raman spectra. Such an advantage of the CP measurements is partially due to a lack of a Rayleigh scattering background and photoluminescence in the pump-probe detection scheme. The weaker intensity of RBMs below 200 cm^{-1} in the

Table 1. The fitted frequency $\omega_{RBM}(\mathrm{cm}^{-1})$, the fitted FWHM $\Gamma_{RBM}(\mathrm{cm}^{-1})$ of RBMs, the theoretical frequency $\omega^{T}_{RBM}(\mathrm{cm}^{-1})$[9,13,37], the transition energy $E^{S}_{22}(\lambda,\mathrm{nm})$, the chirality (n,m), and the chirality type $(n\text{-}m)$ mod 3 of the assigned nanotube. The fitted frequencies of RBMs are consistent with the theoretical value to within $\pm 2.1\ \mathrm{cm}^{-1}$.

$\omega_{RBM}(\mathrm{cm}^{-1})$	$\Gamma_{RBM}(\mathrm{cm}^{-1})$	$\omega^{T}_{RBM}(\mathrm{cm}^{-1})$	$E^{S}_{22}(\lambda,\mathrm{nm})$	(n,m)	$(n\text{-}m)$ mod 3
187.8	1.67	187.2	822	(15,2)	+1
189.3	5.29	191.4	838	(11,7)	+1
197.7	3.09	198.3	795	(12,5)	+1
199.9	1.35	200.8	858	(11,6)	−1
207.1	2.44	207.5	857	(12,4)	−1
212.2	2.55	211.9	859	(13,2)	−1
214.3	3.4	213.6	859	(14,0)	−1
226.0	1.93	225.1	791	(10,5)	−1
233.5	1.25	232.8	792	(11,3)	−1
237.7	3.97	237.0	801	(12,1)	−1

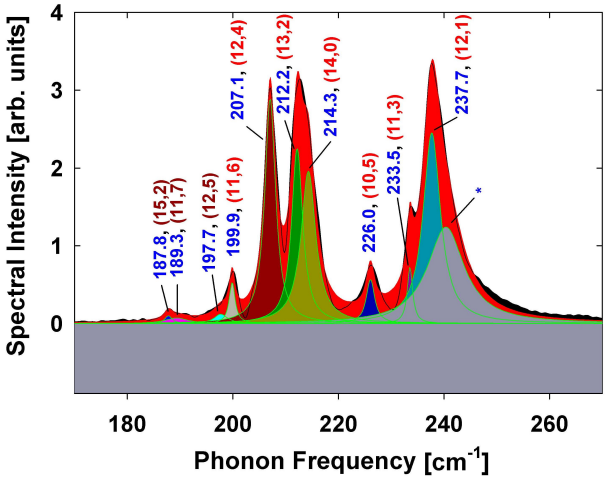

Fig. 4. Peak-fitted radial breathing modes in coherent phonon spectrum using a Lorentzian line shape. Ten radial breathing modes are identified and could be successfully assigned. The reddish-brown color of the assignment labels denotes $(n\text{-}m)$ mod 3 = +1 nanotubes while the red color denotes $(n\text{-}m)$ mod 3 = −1 nanotubes. The blue asterisk denotes the nanotube (or nanotubes) that as of yet are unassigned theoretically, regardless of showing a strong intensity.

CP spectrum as compared to the RRS spectrum is due to the double peak feature of RBMs in the CP spectrum, in which RBMs resonantly excited by femtosecond optical pulses, making their center wavelength equal to the excitonic absorption lines, show rather weaker intensity, as described in our previous work [21].

The narrower line widths in the CP data make it possible to resolve blended peaks in the RRS data. Figure 4 shows RBMs in the CP spectrum peak-fitted with a Lorentzian line shape. The fitting was done using the Peakfit software package (v4.14 Seasolve Software Inc.) by assuming each phonon could be fitted as a Lorentzian peak centered on the radial breathing mode frequency of a specific (n,m) nanotube. The fit was optimized using a minimized residuals method. As Figure 4 shows, we have identified and successfully assigned 10 RBMs in only a single CP spectrum measured by femtosecond pulses with a center wavelength of 830 nm. Table 1 shows the fitted frequency and the corresponding full width at half maximum (FWHM) of RBMs, as well as the theoretical frequency, the chirality, and the corresponding mod type of the assigned nanotubes. When exciting the second excitonic transition energy, E^{S}_{22}, for individual semiconducting nanotubes, $(n\text{-}m)$ mod 3 = −1 nanotubes show markedly stronger intensity than $(n\text{-}m)$ mod 3 = +1 nanotubes, which is consistent with the RRS experimental results [26,27]. As Table 1 shows, the fitted line width of RBMs was ∼2 – 3 cm^{-1}, except for two RBMs affected by unknown neighbor modes at 189 and 238 cm^{-1}, respectively. The linewidths measured in this study for the same HiPco sample using RRS and in other high-resolution CW RRS experiments for different carbon nanotube samples were consistently 5 ∼ 6 cm^{-1} [27–32], excluding the two exceptional cases for isolated SWNTs suspended over a trench and the inner shell tube of double-walled carbon nanotubes, where RRS measured 1.5 cm^{-1} and 1 cm^{-1} [33–35]. Previous studies in bulk semiconductor also indicate that phonon linewidths obtained in CP spectra are sharper than those in CW RRS spectra [25, 36]. Taking into account that both CP and RRS share the same primary decay process of phonon decay into lower-frequency phonon modes through anharmonicity, this discrepancy on the phonon linewidh between CP and RRS is surprising, but more systematic studies of the temperature dependence and interactions with the environment should be done to clarify the discrepancy and to identify the exact decay mechanism for both CP and RRS, as mentioned in our previous study [21].

Among the multiple optical CW spectroscopies developed so far to assign the chirality of carbon nanotubes, photoluminescence shows a primary limitation of being applicable only to semiconducting nanotubes. CW RRS

has been successfully applied to the chirality assignment of nanotubes for both electronic states, but does not exhibit such a sufficient resolution and narrow linewidths to resolve all available blended RBMs as shown in our spectra. Additionally RRS systems of high resolution often have a high purchase cost (excitation source, monochromator, CCD detector, *etc.*). However, CP measurements present several advantages, including excellent resolution and narrow linewidths, no Rayleigh scattering background at low frequency, no photoluminescence signal, and direct measurement of vibrational dynamics, including phase information and decay time, as well as a lower overall system purchase cost (excitation source, optics, delay stage, and photodiode detector). Furthermore, the expansion of the spectrum of femtosecond pulses into deep mid-infrared and visible ranges allows us to investigate large-diameter carbon nanotubes, including metallic nanotubes.

IV. CONCLUSION

Coherent phonon measurements represent a new high-resolution optical spectroscopy allowing accurate assignment of the chiral index of single-walled carbon nanotubes. The amplitude of the lattice vibrations of the radial breathing modes observed in SWNTs was comparable to other bulk semiconductors like GaAs or ZnSe. Almost all available radial breathing modes in the fast Fourier transform of coherent phonon oscillations for individualized SWNTs could be well-resolved with less ambiguity compared to CW resonant Raman scattering.

ACKNOWLEDGMENTS

This work was supported by the Korean Research Foundation Grant, funded by Korean Government (MOEHRD), (KRF-2006-311-C00056) and by Konkuk University.

REFERENCES

[1] S. Iijima and T. Ichihasi, Nature **363**, 603 (1993).
[2] A. Hashimoto, K. Suenaga, A. Gloter, K. Urita and S. Iijima, Nature **430**, 870 (2004).
[3] J. M. Zuo, I. Vartanyants, M. Gao, R. Zhang and L. A. Nagahara, Science **300**, 1419 (2003).
[4] J. W. G. Wildöer, L. C. Venema, A. G. Rinzler, R. E. Smalley and C. Dekker, Nature **391**, 59 (1998).
[5] T. W. Odom, J. L. Juang, P. Kim and C. M. Lieber, Nature **391**, 62 (1998).
[6] J. Park, M. J. Seong, J. Im, M. Lee, S. Myung, S. Hong, H. C. Jo, K. M. Kim and H. Cheong, J. Korean Phys. Soc. **48**, 1347 (2006).
[7] A. M. Rao, E. Richter, S. Bandow, B. Chase, P. C. Eklund, K. W. Williams, S. Fang, K. R. Subbaswamy, M. Menon, A. Thess, R. E. Smalley, G. Dresselhaus and M. S. Dresselhaus, Science **275**, 187 (1997).
[8] A. Hagen and T. Hertel, Nano Lett. **3**, 383 (2003).
[9] S. M. Bachilo, M. S. Strano, C. Kittrell, R. H. Hauge, R. E. Smalley and R. B. Weisman, Science **298**, 2361 (2002).
[10] K. J. Lee, H. Lee, J. Y. Lee, S. C. Lim, H. An, Y. H. Lee and Y. S. Lee, J. Korean Phys. Soc. **46**, 906 (2005).
[11] V. Perebeinos, J. Tersoff and P. Avouris, Phys. Rev. Lett. **94**, 027402 (2005).
[12] C. Thomsen and S. Reich, in *Light Scattering in Solids IX*, edited by M. Cardona and R. Merlin (Springer, Berlin, 2006), Chap. 3.
[13] V. N. Popov, L. Henrard and P. Lambin, Nano Lett. **4**, 1795 (2004).
[14] V. N. Popov, L. Henrard and P. Lambin, Phys. Rev. B **72**, 035436 (2005).
[15] M. Machon, S. Reich, H. Telg, J. Maultzsch, P. Ordejon and C. Thomsen, Phys. Rev. B **71**, 035416 (2005).
[16] S. V. Goupalov, Phys. Rev. B **71**, 153404 (2005).
[17] J. Jiang, R. Saito, A. Gruneis, S. G. Chou, G. G. Samsonidze, A. Jorio, G. Dresselhaus and M. S. Dresselhaus, Phys. Rev. B **71**, 205420 (2005).
[18] S. V. Goupalov, B. C. Satishkumar and S. K. Doorn, Phys. Rev. B **73**, 115401 (2006).
[19] C. Fantini, A. Jorio, M. Souza, M. S. Strano, M. S. Dresselhaus and M. A. Pimenta, Phys. Rev. Lett. **93**, 147406-1 (2004).
[20] S. Reich, C. Thomsen and J. Robertson, Phys. Rev. Lett. **95**, 077402 (2005).
[21] Y. S. Lim, K. J. Yee, J. H. Kim, E. H. Hároz, J. Shaver, J. Kono, S. K. Doorn, R. H. Hauge and E. Smalley, Nano Lett. **4**, 1795 (2006).
[22] M. J. O'Connell, S. M. Bachilo, C. B. Huffman, V. C. Moore, M. S. Strano, E. H. Hároz, K. L. Rialon, P. J. Boul, W. H. Noon, J. Ma, R. H. Hauge, R. B. Weisman and R. E. Smalley, Science **297**, 593 (2002).
[23] G. C. Cho, W. Kutt and H. Kurtz, Phys. Rev. Lett. **65**, 764 (1990).
[24] Y. S. Lim, S. C. Yoon, K. J. Yee, Y. H. Ahn, E. Oh and J. H. Lee, Appl. Phys. Lett. **82**, 2246 (2003).
[25] K. J. Yee, K. G. Lee, E. Oh, D. S. Kim and Y. S. Lim, Phys. Rev. Lett. **88**, 105501 (2002).
[26] J. Jiang, R. Saito, A. Grűneis, S. G. Chou, G. Samsonidze, A. Jorio, G, Dresselhaus and M. S. Dresselhaus, Phys. Rev. B **71**, 45417 (2005).
[27] M. Machon, S. Reich, H. Telg, J. Maultzsch, P. Ordejon and C. Thomsen, Phys. Rev. B **71**, 035416 (2005).
[28] A. Jorio, C. Fantini, M. A. Pimenta, R. B. Capaz, G. G. Samsonidze, G. Dresselhaus, M. S. Dresselhaus, J. Jiang, N. Kobayashi, A. Gruneis and R. Saito, Phys. Rev. B **71**, 075401 (2005).
[29] J. Maultzsch, H. Telg, S. Reich and C. Thomsen, Phys. Rev. B **72**, 205438 (2005).
[30] M. J. O'Connell, S. Sivaram and S. K. Doorn, Phys. Rev. B **69**, 235415 (2004).
[31] A. Jorio, C. Fantini, M. S. S. Dantas, M. A. Pimenta, A. G. Souza Filho, Ge. G. Samsonidze, V. W. Brar, G. Dresselhaus, M. S. Dresselhaus, A. K. Swan, M. S. Unlu, B. B. Goldberg and R. Saito, Phys. Rev. B **66**, 115411 (2002).

[32] A. G. Souza Filho, S. G. Chou, Ge. G. Samsonidze, G. Dresselhaus, M. S. Dresselhaus, L. An, J. Liu, A. K. Swan, M. S. Unlu, B. B. Goldberg, A. Jorio, A. Gruneis and R. Saito, Phys. Rev. B **69**, 115428 (2004).

[33] F. Simon, Á. Kukovecz, Z. Kónya, R. Rfeiffer and H. Kuzmany, Chem. Phys. Lett. **413**, 506 (2005).

[34] R. Pfieffer, F. Simon, H. Kuzmany and V. N. Popov, Phys. Rev. B **72**, 161404 (2005).

[35] H. Kataura, T. Ueno, Y. Miyata, K. Yanagi, S. Okubo, S. Suzuki and Y. Achiba, *Presentation at 20th International Conference on Raman Spectroscopy* (Yokohama, Japan, 2006).

[36] C. Aku-Leh, J. Zhao, R. Merlin, J. Menéndez and M. Cardona, Phys. Rev. B **71**, 205211 (2005).

[37] S. K. Doorn, D. A. Heller, P. W. Barone, M. L. Usrey and M. S. Strano, Appl. Phys. A **78**, 1147 (2004).